

Strong perpendicular anisotropy in $\text{Fe}_{1-x}\text{Co}_x$ alloy films epitaxially grown on mismatching Pd(001), Ir(001), and Rh(001) substrates

F. Yildiz,¹ M. Przybylski,^{1,2,*} X.-D. Ma,¹ and J. Kirschner¹

¹*Max-Planck-Institut für Mikrostrukturphysik, Weinberg 2, 06120 Halle, Germany*

²*Faculty of Physics and Applied Computer Science, AGH University of Science and Technology, al. Mickiewicza 30, 30-059 Kraków, Poland*

(Received 8 May 2009; published 20 August 2009)

In tetragonally distorted $\text{Fe}_{1-x}\text{Co}_x$ alloy films grown epitaxially on Pd(001), Ir(001), and Rh(001) substrates, a strong uniaxial anisotropy and an easy-magnetization axis perpendicular to the film plane are observed. The strongest perpendicular anisotropy is achieved when the $\text{Fe}_{0.5}\text{Co}_{0.5}$ films are grown on Rh(001) ($c/a=1.24$) and it systematically decreases for Ir(001) ($c/a=1.18$) and Pd(001) ($c/a=1.13$) substrates in agreement with the theoretical predictions. For the $\text{Fe}_{1-x}\text{Co}_x$ films grown on Rh(001) the easy-magnetization axis remains perpendicular up to 15 ML in a broad composition range even at room temperature, which is different from the $\text{Fe}_{1-x}\text{Co}_x$ films grown on Pd(001) showing a perpendicular easy-magnetization axis only for $x=0.5$ and only at low temperature. By growing a pseudomorphic buffer layer of Pd on Rh(001) it is shown that the substrate lattice constant and the resulting film distortion are the factors which are decisive for the uniaxial magnetic anisotropy of the $\text{Fe}_{1-x}\text{Co}_x$ films of the same composition.

DOI: [10.1103/PhysRevB.80.064415](https://doi.org/10.1103/PhysRevB.80.064415)

PACS number(s): 75.30.Gw, 75.70.Ak

I. INTRODUCTION

The microscopic origin of and the possibility to manipulate magnetic anisotropy have been of interest for a long time.¹⁻³ Especially, the perpendicular magnetic anisotropy (PMA), which can be sufficiently strong to result in an easy-magnetization axis perpendicular to the film (or multilayer) plane, has been investigated. A variety of applications for magnetic field sensors, magnetic recording, hybrid semiconductor spin electronics, and magneto-optical devices are discussed in literature.⁴⁻⁶ After numerous experimental and theoretical studies, a general understanding of PMA has been achieved. Theoretical studies indicate the important role of the band structure in achieving PMA. In general, an increase in the anisotropy can be expected when the energy separation of the electronic states, one located below and the other above the Fermi level (E_F), will be reduced.⁷ Such situation can occur only for a special symmetry and an appropriate position of E_F , which explains why PMA appears only in a limited combination of metals and a particular crystal orientation. For example, the easy-magnetization axis perpendicular to the sample plane was achieved in multilayer structures such as Co/Pd(111) and Co/Pt(111).⁸⁻¹¹

The concept to achieve a strong PMA in relatively thick 3d metal films refers to the lattice distortion which can result in electronic states located near the Fermi level.¹² A model system is provided by $\text{Fe}_{1-x}\text{Co}_x$ alloy films of cubic structure tetragonally distorted due to their pseudomorphic growth on mismatching substrates. The model predicts a strong uniaxial magnetic anisotropy for a tetragonal distortion with c/a close to 1.22 and E_F which needs to be adjusted to the value ensuring a minimum distance between the occupied and unoccupied states.¹² Since the composition of $\text{Fe}_{1-x}\text{Co}_x$ alloys determines the number of valence electrons, E_F can be varied by a varying the film composition.

The aim of this study is to show that a strong magnetic perpendicular anisotropy in $\text{Fe}_{1-x}\text{Co}_x(001)$ films can be

achieved through an appropriate tetragonal distortion of the film structure. This tetragonal distortion is realized by growing the $\text{Fe}_{1-x}\text{Co}_x$ films on mismatching substrates such as Pd(001), Ir(001), and Rh(001). As their in-plane lattice constants are larger than that of Fe and Co, the lattice of the $\text{Fe}_{1-x}\text{Co}_x$ overlayer has to expand in-plane for pseudomorphic growth. To keep the atomic volume constant, the fcc film contracts in the direction of the c axis, which leads to a c/a ratio less than $\sqrt{2}$, i.e., the value expected for a perfectly cubic fcc structure. A variation in the uniaxial anisotropy within the Pd, Ir, and Rh sequence is observed. In order to exclude any influence of the interface electronic hybridization, a buffer layer of the same material (Pd) was grown pseudomorphically on Rh substrate.

II. EXPERIMENT

The experiments were performed in a multichamber ultra-high vacuum system with a pressure below 2×10^{-10} mbar during Fe and Co deposition. Pd(001) and Rh(001) substrates were prepared with cycles of 1 keV Ar-ion sputtering and subsequent annealing at 900 K. A more complex procedure was applied for the Ir(001) single crystal.^{13,14} The crystal was cleaned by Ar⁺-ion bombardment (ion energy: 2 keV) and subsequent annealing at 1500 K for 10 s. The clean surface was characterized by a quasihexagonal (5×1)Hex reconstruction, as identified by low-energy electron diffraction (LEED). The Ir(001)-(5 \times 1)Hex substrate was then annealed in O₂ at 1400 K for 10 s until an oxygen terminated Ir(001)-(2 \times 1)-O reconstruction was observed in LEED. The Ir(001)-(1 \times 1) surface was finally obtained by subsequently exposing the Ir(001)-(2 \times 1)-O layer to H₂ at 400 K. This preparation resulted in a Ir(001)-(1 \times 1) surface, as checked by LEED, and this surface was used as a template for epitaxial growth of the $\text{Fe}_{1-x}\text{Co}_x$ layers.

The quality of the crystal surfaces was checked by Auger electron spectroscopy (AES) and by scanning tunneling mi-

croscopy (STM) until a clean surface with nearly equidistant and parallel monoatomic steps was obtained. The Fe-Co films were grown at room temperature (RT) by molecular beam epitaxy from the effusion cells. The Pd and Rh buffer layers were grown from rods of high purity by electron bombardment. LEED was used to quantitatively assess the pseudomorphic growth, and STM to verify the film topology, in particular, for Pd buffer layers grown on Rh(001).

Magnetic properties were probed by utilizing the *in situ* magneto-optical Kerr effect (MOKE) for a 1.85 eV photon energy of *s*-polarized light, a beam diameter <0.4 mm, mostly in polar geometry (incidence angle of 69° to the sample normal) at varying temperature (down to 5 K) and the external magnetic field up to 0.7 T.

III. RESULTS AND DISCUSSION

In order to analyze the uniaxial magnetic anisotropy in tetragonally distorted $\text{Fe}_{1-x}\text{Co}_x$ films systematically, we have chosen to grow the films on a (001) surface of three different crystals: Rh, Ir, and Pd. The in-plane lattice constant of the crystals increases in the following sequence: Rh (2.69 Å), Ir (2.72 Å), and Pd (2.75 Å).

A. Anisotropy vs lattice constant

$\text{Fe}_{1-x}\text{Co}_x$ films were grown on a Rh(001) substrate at RT. To quantitatively assess the amount of tetragonal distortion, both diffraction intensity vs electron energy analysis [I(V)-LEED] and Kikuchi patterns of quasielastically backscattered electrons were performed. We observed almost perfect pseudomorphic epitaxial growth up to a thickness of at least 12 ML depending on the film composition, with a c/a ratio around 1.24.¹⁵

We found that $\text{Fe}_{1-x}\text{Co}_x$, $0.3 < x < 0.65$, alloy films grown on Rh(001) show a clear out-of-plane easy axis of magnetization at RT, i.e., rectangular polar MOKE loops were measured up to a thickness of $d_c = 15$ ML (Fig. 1). Since pure Fe and Co films grown on Rh(001) are spontaneously magnetized in plane independently of their thickness,¹⁶⁻¹⁸ it is reasonable to assume that both the surface and the Fe-Co/Rh interface effects do not contribute significantly to the perpendicular anisotropy, e.g. of the $\text{Fe}_{0.5}\text{Co}_{0.5}/\text{Rh}(001)$ system. Thus we interpret the perpendicular easy-magnetization axis as a result of a strong magnetocrystalline anisotropy which is directly related to the tetragonal distortion. A clear perpendicular easy-magnetization axis is observed up to 390 K, i.e., the maximum temperature applied by us. The uniaxial magnetic anisotropy is much stronger than the shape anisotropy of the $\text{Fe}_{0.5}\text{Co}_{0.5}$ film, thus the easy-magnetization axis is well defined and not sensitive to increasing temperature.

Previously, a different behavior was observed for $\text{Fe}_{1-x}\text{Co}_x$ films grown on Pd(001).¹⁹ For this system the tetragonal distortion c/a is equal to 1.13, i.e. much less than the $c/a = 1.24$ obtained for films of the same composition and thickness but grown on Rh(001). We found that the uniaxial anisotropy of $\text{Fe}_{0.5}\text{Co}_{0.5}$ films on Pd(001) is of the same order as the shape anisotropy, resulting in a small but positive effective anisotropy energy, i.e., forcing the easy-

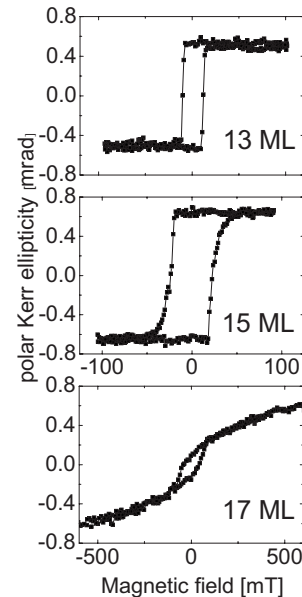


FIG. 1. Polar hysteresis loops measured at RT for $\text{Fe}_{0.4}\text{Co}_{0.6}$ films of varying thickness grown on Rh(001). The loops are rectangular up to a thickness of 15 ML

magnetization axis to be oriented perpendicular to the film plane. Interestingly enough, the perpendicular easy-magnetization axis was detected only for compositions around $x=0.5$ and only at low temperatures (LT).¹⁹ The surface anisotropy was found to be negative in this case, i.e., forcing the magnetization to be oriented in the sample plane. Thus a positive effective anisotropy (i.e., an easy-magnetization axis perpendicular to the sample plane) was observed above a thickness of 4 ML only. To us this finding is plausible since the tetragonal distortion of $\text{Fe}_{0.5}\text{Co}_{0.5}$ films grown on Pd(001) is on the order of $c/a = 1.13$ for which the uniaxial anisotropy is predicted to be much smaller than for films of the same composition grown on Rh(001) (i.e., of $c/a = 1.24$).¹²

In order to make the analysis more complete, we performed a MOKE experiment with $\text{Fe}_{1-x}\text{Co}_x$ films grown on Ir(001) [$c/a = 1.18$ (Ref. 20)]. Similarly to Pd(001)¹⁹ and Rh(001)¹⁵ the measurements revealed that the easy-magnetization axis is in plane for Fe and Co layers on Ir(001), at least above a thickness of 5 ML.^{14,21} For $\text{Fe}_{1-x}\text{Co}_x$ around an $x=0.5$ composition, the easy-magnetization axis is found perpendicular to the sample plane even at RT. The effective anisotropy for a $\text{Fe}_{0.5}\text{Co}_{0.5}$ film grown on Ir(001), i.e., less distorted ($c/a = 1.18$) than films of the same composition grown on Pd(001) ($c/a = 1.13$), is expected to be larger.¹² The polar Kerr ellipticity loops measured for 9- and 15-ML-thick films of $\text{Fe}_{0.5}\text{Co}_{0.5}$ on an Ir(001) substrate at RT (Fig. 2) clearly prove these findings. The loops are rectangular and show a 100% magnetization in remanence both at RT and at LT, which confirms that the easy-magnetization axis is oriented perpendicular to the film plane. Only when the thickness exceeds 15 ML, e.g., for 18 ML as shown in Fig. 2, the loops identify the easy-magnetization axis as switching to the sample plane. $\text{Fe}_{1-x}\text{Co}_x$ films grown on Ir(001) show the properties somewhere in between the properties observed

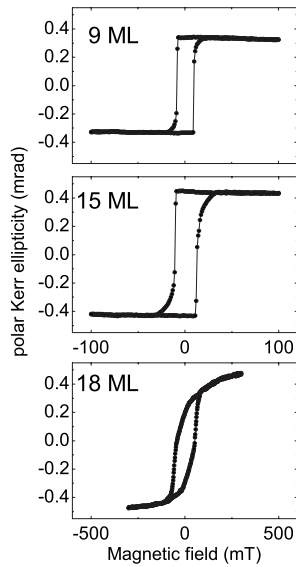


FIG. 2. Polar hysteresis loops measured at RT for Fe_{0.5}Co_{0.5} films of varying thickness grown on Ir(001).

for Fe_{1-x}Co_x films grown on Pd(001) and those grown on a Rh(001) substrate.

It is worthwhile to mention that Fe_{0.5}Co_{0.5} films grown on Rh(001), Ir(001), and Pd(001) show an easy-magnetization axis perpendicular to the sample plane up to almost the same thickness (of about 15 ML) in all three cases. However, the films grown on Pd(001) exhibit a perpendicular magnetization only at LT. The thickness up to which the easy-magnetization axis is kept perpendicular to the film plane is not directly related to the strength of the anisotropy. In principle, the perpendicular magnetocrystalline anisotropy, being larger than the shape anisotropy, is sufficient to keep the easy-magnetization axis perpendicular to the film independently of the film thickness. The thickness at which the magnetization starts to rotate toward the film plane (d_c) is mainly determined by the thickness up to which the tetragonal distortion (d_t) is kept. Above d_t the distortion starts to relax, the configuration of the crystal field changes and the strong uniaxial anisotropy disappears. However, the thickness range necessary to balance the perpendicular magnetocrystalline anisotropy with the shape anisotropy, $d_c - d_t$, depends on the strength of the perpendicular anisotropy. Thus some composition dependence of d_c can be observed.^{15,22}

Fe_{1-x}Co_x films were also grown on Pt(001).²³ However, here the perpendicular anisotropy was not strong enough to over-ride dipolar interactions and to result in a perpendicular easy-magnetization axis at RT. Differently to our films, the multilayer was grown with Fe_{0.5}Co_{0.5} having a film thickness of only 3 ML repeated for many times within the Fe_{0.5}Co_{0.5}/Pt sequence.

B. Anisotropy vs temperature

The volume magnetocrystalline anisotropy for Fe_{0.5}Co_{0.5} films on Pd(001) is found to be strongly temperature dependent. As it is shown in Fig. 3, the polar Kerr ellipticity loops measured at 5 and 50 K are rectangular showing 100% satu-

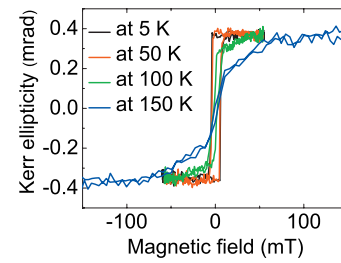


FIG. 3. (Color) Polar hysteresis loops for 6 ML of Fe_{1-x}Co_x on Pd(001) at different temperatures. The rectangular easy-axis-like loop measured at 5 K evolves to the hard-axis-like loop when measured above 100 K (i.e., the SRT occurs between 50 and 100 K).

ration magnetization in remanence. The loops measured at 100 K and above show a nonrectangular hard-axis-like shape and zero magnetization in remanence when measured at 150 K. This means that the temperature-driven spin reorientation transition (SRT) occurs at a temperature range between 50 and 100 K. Moreover, it also confirms that the uniaxial/perpendicular magnetocrystalline anisotropy is only a little larger than the shape anisotropy and can thus be easily overridden by a slightly increasing temperature.

Unlike the films grown on Pd(001) the Fe_{1-x}Co_x films grown on Rh(001) do not show any temperature dependence of the anisotropy resulting in SRT. This is due to the much stronger magnetocrystalline uniaxial anisotropy of Fe_{1-x}Co_x films when grown on a Rh(001) substrate. The reason is that here the in-plane lattice constant of Fe_{1-x}Co_x films is less expanded. Thus, the interlayer distance contracts less to keep the volume unchanged, and a much larger c/a ratio of 1.24 is finally achieved.¹⁵ The increasing temperature affects the magnetocrystalline anisotropy which is thereby smaller, but still much larger than the shape anisotropy.

The situation is shown schematically in Fig. 4, in which we plot the uniaxial anisotropy energy, K_u , with reference to the dipolar (shape) anisotropy. The composition dependen-

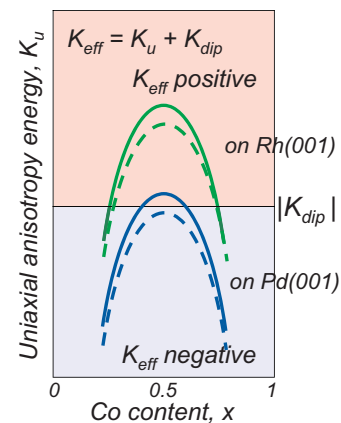


FIG. 4. (Color) Schematic representation of the effective anisotropy with respect to the shape anisotropy energy for Fe_{1-x}Co_x films grown on Pd(001) and Rh(001). Solid lines correspond to the anisotropy energy balance at LT (60 K), dotted lines at RT. The figure explains why the increasing temperature has almost no effect on the easy-magnetization axis for Fe_{1-x}Co_x films grown on Rh(001), whereas it results in SRT for Fe_{0.5}Co_{0.5} film grown on Pd(001).

cies of K_u show only a general trend following the dependencies precisely given in Ref. 12. The values above $|K_{dip}|$ refer to the positive effective anisotropy constant and resulting easy magnetization axis perpendicular to the film plane, whereas the values below $|K_{dip}|$ refer to the in-plane magnetization. The anisotropy energy is plotted vs. the film composition at two different temperatures (RT and LT) for both systems, i.e., for $Fe_{1-x}Co_x$ films grown on Pd(001) and Rh(001). From the diagram it can be easily understood how and why the easy-magnetization axis depends both on temperature and film composition. By assuming qualitatively the same dependence of K_u on the composition at RT and LT, it can be seen immediately that a tiny reduction in K_u results in a negative volume anisotropy for the $Fe_{1-x}Co_x/Pd(001)$ system independently of the film composition (Fig. 4) and the film thickness.²⁰

In the case of distorted films grown on mismatching substrates, the crystallographic distortion (responsible for the uniaxial magnetocrystalline anisotropy) can be thickness dependent. Obviously, the effective anisotropy changes as the thickness of the film structure relaxes (at d_t), and the uniaxial magnetic anisotropy becomes weaker than the shape anisotropy (at d_c). Since the anisotropy is temperature dependent (this is simply because the ferromagnetic order is temperature dependent), the increasing temperature reduces the uniaxial anisotropy. But it has almost no influence on the easy-magnetization axis of the $Fe_{0.5}Co_{0.5}$ films grown on Rh(001), because the uniaxial magnetic anisotropy is much larger in this case than the shape anisotropy. For $Fe_{0.5}Co_{0.5}$ films grown on Pd(001), the effective anisotropy is small, i.e., the uniaxial magnetocrystalline is only a little larger than the shape anisotropy, yet still positive—at least at LT. The anisotropy changes only a little with increasing temperature, however, the change is sufficient to result in a negative effective anisotropy (the uniaxial magnetocrystalline anisotropy becomes smaller than the shape anisotropy as it is usually observed for most ultrathin films).

In summary, at RT $Fe_{0.5}Co_{0.5}$ films grown on Rh(001) are spontaneously magnetized perpendicular to the sample plane, whereas films of the same composition grown on Pd(001) are magnetized in the sample plane. We attribute this different magnetic anisotropy to the different tetragonal distortion of the $Fe_{1-x}Co_x$ overlayers due to the different in-plane lattice constant of the Rh(001) and Pd(001) substrates. Conversely, we argue that the magnetic anisotropy for films of the same composition depends only on the lattice constant of the substrate (which, however, must allow the $Fe_{1-x}Co_x$ film to grow pseudomorphically to the substrate). This is also in agreement with theoretical predictions.¹²

C. Anisotropy with a buffer layer

In order to exclude any influence of the substrate's electronic structure on the anisotropy of the overlayer, we have grown a $Fe_{0.5}Co_{0.5}$ film on a buffer layer of Pd a few ML thick on top of the Rh(001) substrate. The idea was to grow the $Fe_{0.5}Co_{0.5}$ film on top of a well-ordered single crystalline layer of a material which is chemically different from Rh but has exactly the same lattice constant as the Rh(001) sub-

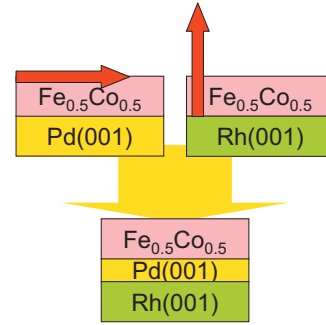


FIG. 5. (Color) Schematic depiction of the MOKE experiment, where $Fe_{0.5}Co_{0.5}$ films on a Pd buffer layer are grown on Rh(001) substrate.

strate. Pd was chosen as a buffer layer due to its expected epitaxial growth on the Rh(001) substrate. Moreover, the magnetic properties of the $Fe_{1-x}Co_x$ films grown on a single crystalline Pd(001) surface had been well established previously¹⁹ and were easy to compare.

The idea of this experiment is shown schematically in the Fig. 5: at RT the $Fe_{0.5}Co_{0.5}$ films are magnetized in plane when grown on Pd(001) (the magnetization rotates to the film normal only at low temperature), whereas they are magnetized perpendicular to the film plane when grown on Rh(001). The films of a different composition, such as $x = 0.4$, are magnetized in plane when grown on Pd(001), and perpendicular to the film plane when grown on Rh(001), independently of temperature. When the $Fe_{1-x}Co_x$ film is grown on top of the Pd buffer layer, its magnetic properties should reflect the origin of the perpendicular anisotropy: either the electronic structure of the substrate (i.e., of Pd) or a tetragonal distortion due to the mismatching lattice constant (i.e., that of Rh). As a result, the easy-magnetization axis should be oriented in plane or perpendicular to the sample plane, respectively.

In Fig. 6 we show STM images of Pd films grown at RT on the Rh(001) substrate. It can be clearly seen that at RT the growth is almost perfect layer by layer. The second and all other atomic layers do not start to form before the previous layer is not complete. This is confirmed by the thickness profile taken along the line indicated in the STM image of 4.4 ML of Pd. The free surface energy of Pd is 2.1 J/cm^2 and smaller than the free surface energy of Rh of 2.75 J/cm^2 , i.e., $\gamma_{Pd} < \gamma_{Rh}$.²⁴ Thus, from a thermodynamical perspective the layer-by-layer growth is not a surprise. Such growth supports pseudomorphism and the growing layer can keep the in-plane lattice constant of the substrate up to a thickness of several monolayers.²⁵

The LEED pattern shows (Fig. 7) the spots exactly at the same positions as for the clean Rh(001) substrate, which proves that the lattice constant of the Pd buffer is identical to the lattice constant of Rh(001). It proves the almost ideal pseudomorphic growth of Pd on Rh(001) at least up to 5 ML. AES experiments utilizing the low-energy Auger electrons confirm that Pd-Rh alloying does not exist—at least above the AES detection limit. Thus the Pd buffer layer can be considered to consist of Pd atoms separated in plane with the lattice constant of Rh.

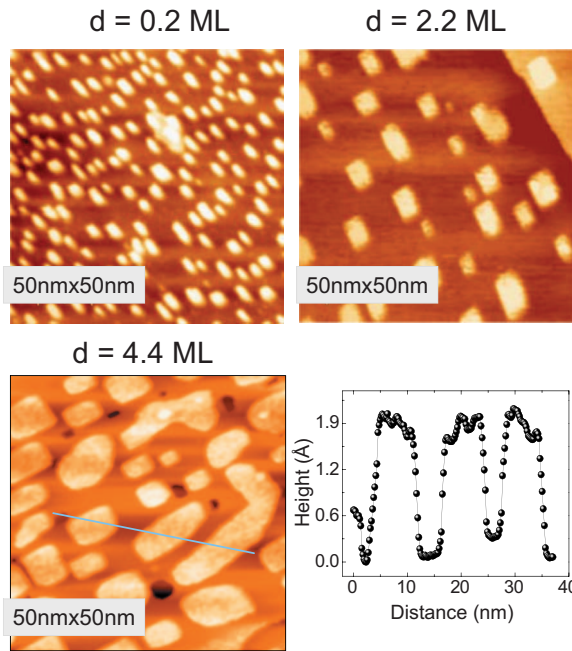


FIG. 6. (Color) STM images of Pd layers of different thickness grown at RT on Rh(001). The line profile is taken as indicated in the STM image for the coverage of 4.4 ML. Almost perfect layer-by-layer growth allows the formation of a continuous and uniformly thick Pd film of a few ML.

Finally, $\text{Fe}_{0.5}\text{Co}_{0.5}$ films were grown on top of such a Pd buffer layer. The deposition was performed at RT and the thickness of the film varied between 6 to 15 ML. The mode of growth was not found to be remarkably different from the growth of the $\text{Fe}_{1-x}\text{Co}_x$ films of the same composition directly on the Rh(001) substrate (see Sec. III A). Polar Kerr ellipticity loops measured for the $\text{Fe}_{0.5}\text{Co}_{0.5}/\text{Pd}/\text{Rh}(001)$ system at RT are shown in Fig. 8. The loops are typical easy-axis loops, being rectangular and showing 100% saturation magnetization in remanence up to 9 ML, which correspond clearly to the easy-magnetization axis perpendicular to the film plane. The hysteresis loops of the $\text{Fe}_{0.5}\text{Co}_{0.5}$ films grown on top of Pd/Rh(001) are exactly the same as the loops measured for the $\text{Fe}_{0.5}\text{Co}_{0.5}$ films grown directly on the Rh(001) substrate. The same applies for films with a composition varying between $x=0.4$ and 0.6. Yet the loops totally differ from the hard-axis loops measured at RT for the

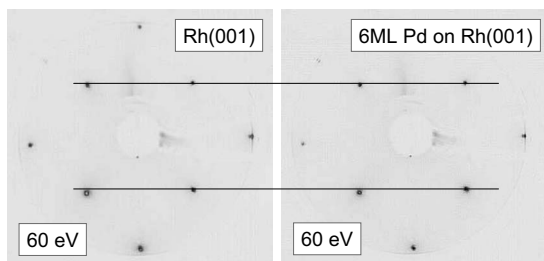


FIG. 7. LEED patterns of (a) the clean Rh(001) substrate and (b) after 6 ML of Pd are grown on top of Rh(001). The patterns are identical in both cases. This confirms the epitaxial growth of the Pd layer pseudomorphic to the Rh(001) substrate.

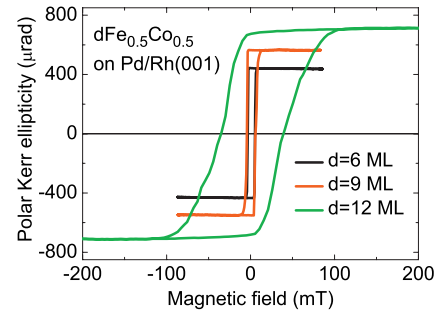


FIG. 8. (Color) Polar Kerr ellipticity loops measured at RT for $\text{Fe}_{0.5}\text{Co}_{0.5}$ films of varying thickness grown on Pd buffer/Rh(001). The films are magnetized out of plane just like the $\text{Fe}_{0.5}\text{Co}_{0.5}$ films grown directly on Rh(001). The easy-magnetization axis perpendicular to the film plane is maintained to a thickness of at least 12 ML.

$\text{Fe}_{0.5}\text{Co}_{0.5}$ films grown on Pd(001).¹⁹ Even the thickness d_c up to which the perpendicular easy magnetization can be kept seems to be more or less identical (around 12 ML) to the one for $\text{Fe}_{0.5}\text{Co}_{0.5}$ films grown on Rh(001). Taking the d_c thickness as a measure of tetragonal distortion, we can conclude that the distortion for $\text{Fe}_{0.5}\text{Co}_{0.5}$ films grown both on Pd/Rh(001) and on Rh(001) is very similar.

Another phenomenon relates to the shape and the increased coercivity of the polar Kerr ellipticity loop measured for a $\text{Fe}_{0.5}\text{Co}_{0.5}$ film 12 ML thick. The loop is no longer rectangular, however, the remanence still equals 100% of the saturation magnetization, and the magnetization starts to re-orient almost at the same field. A very similar observation was made for $\text{Fe}_{1-x}\text{Co}_x$ films of the same composition (i.e., $x=0.5$) grown directly on Rh(001) (compare to Fig. 1). This is most likely due to the different anisotropy energy balance which determines the magnetization switching in the films above the thickness up to which the uniaxial anisotropy dominates. With a decreasing perpendicular anisotropy, the shape anisotropy forces the magnetization to be oriented in the sample plane. Thus more field needs to be applied perpendicular to the sample plane to fully switch and saturate the magnetization.²⁶ The field which is necessary to saturate the sample is much larger (around 100 mT) than the coercivity (and the saturation field) of the $\text{Fe}_{0.5}\text{Co}_{0.5}$ films thinner than 10 ML (around 5 mT).

A reversed system, i.e., a Rh buffer layer on Pd(001), cannot be grown and tested since Rh does not grow layer by layer. STM images show a three-dimensional growth even at low coverage. This is not surprising even from the thermodynamical point of view since the surface energy of Rh is larger than that of Pd ($\gamma_{\text{Rh}} > \gamma_{\text{Pd}}$).²⁴ Moreover, the LEED pattern is not visible before a thickness of at least 7 ML is reached (the maximum thickness of the Rh buffer layer we tested), and an epitaxial growth of the Rh buffer layer on the Pd(001) substrate cannot be confirmed.

The result of the MOKE experiment on the $\text{Fe}_{0.5}\text{Co}_{0.5}/\text{Pd}$ buffer/Rh(001) confirms that the strong perpendicular anisotropy of $\text{Fe}_{0.5}\text{Co}_{0.5}$ films originates from their appropriate tetragonal distortion. From the reported experiments, magnetic anisotropy in $\text{Fe}_{1-x}\text{Co}_x$ films of the same composition (the same x) can be concluded that there exists only a depen-

dence on the c/a ratio, i.e., on how much the film structure is tetragonally distorted. In turn, the distortion is directly related to the lattice mismatch between the material of the film and the substrate. The tetragonal distortion obtained for $\text{Fe}_{0.5}\text{Co}_{0.5}$ films grown on Rh(001) is the most appropriate among the tested substrates in order to get a maximum perpendicular anisotropy. In general, it can be stated that the largest uniaxial magnetic anisotropy can be obtained by growing $\text{Fe}_{0.5}\text{Co}_{0.5}$ films on fcc substrates of the Rh lattice constant. In particular, it can be a pseudomorphic buffer layer of any material epitaxially grown on the Rh(001) substrate since the property which matters is the in-plane lattice constant. In particular, when Pd is grown as a pseudomorphic buffer layer on the mismatching Rh(001) substrate, its lattice constant relates to the lattice constant of the Rh substrate (and not of Pd). Consequently, the achieved uniaxial anisotropy has nothing to do with the anisotropy expected for $\text{Fe}_{1-x}\text{Co}_x$ film grown on a Pd(001) substrate, and reflects what is expected for films grown on Rh(001). This is in agreement with theoretical calculations predicting the largest uniaxial anisotropy for a film of such composition to be about $x=0.5$ and a distortion similar to that observed experi-

mentally for $\text{Fe}_{1-x}\text{Co}_x$ films grown on Rh(001).¹²

D. Conclusions

An appropriate tetragonal distortion and a proper adjustment of the Fermi level result in a strong uniaxial anisotropy in $\text{Fe}_{0.5}\text{Co}_{0.5}$ films grown on Rh(001). An easy-magnetization axis perpendicular to the film plane is kept up to the thickness of 15 ML due to the distortion ($c/a=1.24$), which is unrelaxed up to more than 12 ML. The uniaxial magnetic anisotropy is systematically weaker for Ir(001) ($c/a=1.18$) and Pd(001) ($c/a=1.13$) substrates and systematically depends on the decreasing lattice mismatch between the film and the substrate. By growing $\text{Fe}_{0.5}\text{Co}_{0.5}$ films on buffer layers of Pd on Rh(001), it is shown that the lattice constant of the substrate (and resulting film distortion) is the decisive factor for the uniaxial magnetic anisotropy.

ACKNOWLEDGMENT

The authors would like to thank H. Menge and G. Kroder for their technical support.

*mprzybyl@mpi-halle.mpg.de

¹Ch. Kittel, Phys. Rev. **73**, 155 (1948).

²D. Weller, J. Stöhr, R. Nakajima, A. Carl, M. G. Samant, C. Chappert, R. Megy, P. Beauvillain, P. Veillet, and G. A. Held, Phys. Rev. Lett. **75**, 3752 (1995).

³G. Laan, J. Phys.: Condens. Matter **10**, 3239 (1998).

⁴J. P. J. Groenland, C. J. M. Egkel, J. H. J. Fluitman, and R. M. de Ridder, Sens. Actuators, A **30**, 89 (1992).

⁵D. J. Monsma, J. C. Lodder, Th. J. A. Popma, and B. Dieny, Phys. Rev. Lett. **74**, 5260 (1995).

⁶S. A. Wolf, D. D. Awschalom, R. A. Buhrman, J. M. Daughton, S. Von Molnar, M. L. Rouker, A. Y. Chtchelkanova, and D. M. Treger, Science **294**, 1488 (2001).

⁷P. Bruno, Phys. Rev. B **39**, 865 (1989).

⁸P. F. Carcia, J. Appl. Phys. **63**, 5066 (1988).

⁹B. N. Engel, C. D. England, R. A. Van Leeuwen, M. H. Wiedmann, and C. M. Falco, Phys. Rev. Lett. **67**, 1910 (1991).

¹⁰F. J. A. den Broeder, W. Hoving, and P. J. H. Bloemenet, J. Magn. Magn. Mater. **93**, 562 (1991).

¹¹N. Nakajima, T. Koide, T. Shidara, H. Miyauchi, H. Fukutani, A. Fujimori, K. Iio, T. Katayama, M. Nyvlt, and Y. Suzuki, Phys. Rev. Lett. **81**, 5229 (1998).

¹²T. Burkert, L. Nordström, O. Eriksson, and O. Heinonen, Phys. Rev. Lett. **93**, 027203 (2004).

¹³V. Martin, W. Meyer, C. Giovanardi, L. Hammer, K. Heinz, Z. Tian, D. Sander, and J. Kirschner, Phys. Rev. B **76**, 205418 (2007).

¹⁴Z. Tian, D. Sander, and J. Kirschner, Phys. Rev. B **79**, 024432

(2009).

¹⁵F. Yildiz, F. Luo, C. Tieg, R. M. Abrudan, X. L. Fu, A. Winkelmann, M. Przybylski, and J. Kirschner, Phys. Rev. Lett. **100**, 037205 (2008).

¹⁶K. Hayashi, M. Sawada, H. Yamagami, A. Kimura, and A. Kakizaki, Physica B **351**, 324 (2004); K. Hayashi, M. Sawada, H. Yamagami, A. Kimura, and A. Kakizaki, J. Phys. Soc. Jpn. **73**, 2550 (2004).

¹⁷K. Hayashi, M. Sawada, A. Harasawa, A. Kimura, and A. Kakizaki, Phys. Rev. B **64**, 054417 (2001).

¹⁸M. A. Tomaz, E. Mayo, D. Lederman, E. Hallin, T. K. Sham, W. L. O'Brien, and G. R. Harp, Phys. Rev. B **58**, 11493 (1998).

¹⁹A. Winkelmann, M. Przybylski, F. Luo, Y. Shi, and J. Barthel, Phys. Rev. Lett. **96**, 257205 (2006).

²⁰F. Yildiz, M. Przybylski, J. Kirschner, J. Appl. Phys. **105**, 07E129 (2009).

²¹M. Henkel, S. Andrieu, P. Bauer, and M. Piecuch, Phys. Rev. Lett. **80**, 4783 (1998).

²²F. Luo, X.-L. Fu, A. Winkelmann, and M. Przybylski, Appl. Phys. Lett. **91**, 262512 (2007).

²³G. Andersson, T. Burkert, P. Warnicke, M. Björck, B. Sanyal, C. Chacon, C. Zlotea, L. Nordström, P. Nordblad, and O. Eriksson, Phys. Rev. Lett. **96**, 037205 (2006).

²⁴A. R. Miedema and J. W. F. Dorleijn, Surf. Sci. **95**, 447 (1980).

²⁵U. Gradmann, Surf. Sci. **13**, 498 (1969).

²⁶W. C. Lin, C. C. Kuo, C. L. Chiu, and M.-T. Lin, J. Appl. Phys. **89**, 7139 (2001).